Fracture evolution in small punch tests under constant deflection rate conditions

Petr Dymáček[1a], Karel Milička[1b] and Vojtěch Hrubý[2c]

[1]Institute of Physics of Materials, Academy of Sciences of CR, Žižkova 22, 616 62 Brno, Czech Republic

[2]University of Defense, Faculty of Military Technologies, Department of Mechanical Engineering, Kounicova 65, 612 00 Brno, Czech Republic

[a]pdymacek@ipm.cz, [b]milicka@ipm.cz, [c]vojtech.hruby@unob.cz

Keywords: small punch test, fracture, chromium steel, finite element method.

Abstract. The small punch tests (SPT) can serve similarly as conventional tensile tests for determining of the static mechanical properties, the estimation of fracture toughness and transitions in material behavior. A set of three steels of various ductility has been selected and tested using SP technique at room temperature with constant deflection rate conditions. Evolution of fracture was investigated on specimens tested up to certain levels of deflection and consequently analyzed by light metallography. The localization of cracks and their observed forms are discussed and compared with the stress and strain distributions in the finite element (FE) model of the SPT. Conclusions of the investigation should help to better understanding of the fracture mechanisms that occur in SP testing of materials with great differences in ductility.

Introduction

Small punch tests (SPT) are using specimens of a thin disc shape prepared from a small amount of material that can be extracted directly from the surface of in service parts of facilities without their substantial damage. Therefore, SPT are often classified as the NDE procedures. In these tests, a puncher penetrates through the disc specimen into a hole. Two variations of this test type seem to have a good potential for use in wide range of temperatures. First, the test in which the puncher penetrates through the disc at a given constant rate of deflection (i.e., central deflection measured in a direction perpendicular to the disc) and the necessary force is measured; this test is marked as CDR (constant deflection rate). It has certain analogy with the conventional tensile test. Second, the CF test (constant force) is a test in which the puncher penetrates under constant load and the time dependence of the deflection is measured. This test is similar to a conventional creep test. Both tests are run up to the rupture of the disc. As a rule, the puncher is a ceramic ball or a bar with a hemispherical tip. In an application within the field of power generation or thermal industry, these tests should be performed at elevated temperatures and in a protective atmosphere (argon). A scheme showing the punching arrangement applicable for both test types is illustrated in Fig. 1. Dimensions of the specimen and the arrangement are shown in Table 1. At IPM there is good experience with both types of SP testing, namely for advanced steels, aluminum and magnesium alloys. This technique was also applied to describe the properties of entire welds [1,2]. Recently, there has been an effort to standardize the SPT on European level which is summarized in [3].

Table 1: SPT dimensions

Disc diameter D [mm]	Disc thickness t [mm]	Lower die diameter d [mm]	Puncher ball diameter R [mm]	Radius (or chamfer) r [mm]
8	0.5 ± 0.005	4	1.25	0.2 (0.2)

Present study was aimed at the SP-CDR at room temperature from both experimental and modeling aspects. One of the aims was to compare the differences of disc behavior at brittle and ductile damage and its relation to the measured SPT curves. A typical relation between load and deflection for ductile metals is shown in Fig 2. It can be divided to several parts as described by Abendroth and Kuna [4]. Part I is mainly defined by the elastic material properties, part II represents transition between elastic and plastic material behavior, part III shows the hardening properties up to part IV, where geometrical softening and damage occurs, in part V the penetration of the specimen occurs and part VI represents the remaining force needed to push the puncher through the already ruptured specimen.

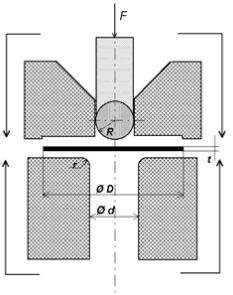

Fig. 1: Scheme of SPT setup

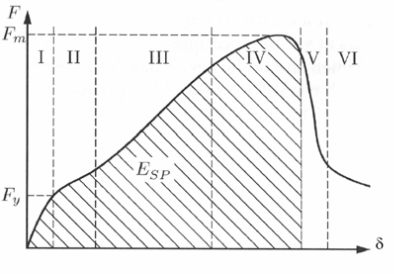

Fig. 2: Typical SPT load-deflection diagram, the dashed area serves to determining of the SP energy E_{SP}

Materials and procedures

For the investigation were selected following three steels:

- low alloyed heat resistant steel type CSN 15313 (EN equivalent 10CrMo9-10). The thermal treatment was normalization heating (940 °C/45 min) and consequent tempering (680 °C/2 h).
- high chromium heat resistant steel P91 (EN equivalent 10216-2). Specimens were prepared from a pipe with an outer radius of 165 mm and a wall thickness of 16 mm. The heat treatment was normalization (1050 °C/1 h) followed by tempering (760 °C/2 h).
- carbon steel of type CSN 12060 (EN equivalent C55). The thermal treatment was quenching and tempering, the exact temperatures and times were not precisely known as the material was extracted from a section of artillery ammunition.

The chemical compositions of all steels are summarized in Table 2.

Table 2: Chemical composition in wt. %

Steel	C	Cr	Mn	Mo	Ni	P	Si	V	Cu	S	Nb	N
CSN 15313	0.10	2.50	0.60	0.90	-	0.025	0.10	-	-	-	-	-
P91	0.10	8.50	0.40	0.88	0.10	-	-	0.23	-	-	0.10	0.045
CSN 12060	0.55	-	0.62	-	-	0.015	0.38	-	0.11	0.027	-	-

Necessary mechanical properties were determined for the CSN 15313 and P91 steels by tensile tests of set of six conventional specimens at room temperature. The speed of loading was 1 mm/min, the test time until rupture was around 10 minutes. Table 3 contains the values of true σ and ε used in the FE model. The CSN 12060 steel was tested only by SPT. Other material properties of the specimen, lower and upper die and ceramic puncher ball are summarized in Table 4.

The SPT was performed on sets of 5 specimens at loading velocities ranging from 10^{-2} to 10^{-6} mm/s until bursting of the disc. Other set of specimens was subjected to tests interrupted at selected deflections for observations of the initiation and development of the cracking.

Table 3a: Values of real stress-strain diagram of CSN 15313 steel obtained by conventional tensile test at 20 °C

ε	0.0	0.002087	0.005	0.01	0.02	0.03	0.04	0.05	0.10	0.15	1.00
σ [MPa]	0.0	430.0	434.3	439.1	470.6	507.4	538.3	563.2	632.6	666.5	1189.7

Table 3b: Values of real stress-strain diagram of P91 steel obtained by conventional tensile test at 20 °C

ε	0.0	0.001779	0.005	0.01	0.02	0.03	0.04	0.05	0.10	0.15	1.00
σ [MPa]	0.0	397	403.1	431.8	489.5	537.0	574.5	604.0	686.2	725.3	1120.7

Table 4: Mechanical properties applied in the FE model

	Young modulus E **[GPa]**	**Poisson const.** ν **[–]**	**Yield stress** R_e **[MPa]**
CSN 15313 (at 20 °C)	206	0.3	430
P91 (at 20 °C)	223	0.3	397
lower and upper die	210	0.3	–
ceramic ball (99.7% Al_2O_3)	370	0.22	–

Numerical model

The numerical model of SPT shown in Fig. 3 was formulated in the finite element system ANSYS, see [5] for more details. The model consisted of 1624 axisymmetric elements PLANE182 and the contact surfaces were defined by CONTA171 and TARGE169 elements. Geometrical and material characteristics can be input as parameters to the model. Boundary conditions were applied as close as possible to reality, i.e. vertical displacement $u_y = 0$ on the lower and upper die ends. The load was applied as vertical displacement of the puncher. Solution of the task was performed by sparse direct solver in the range of the puncher displacement 0 to 2 mm divided on 2000 sub-steps. The numerical model did not contain any representation of damage or fracture.

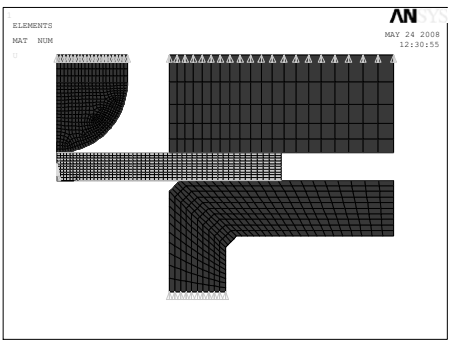

Fig. 3: FE model of SPT setup

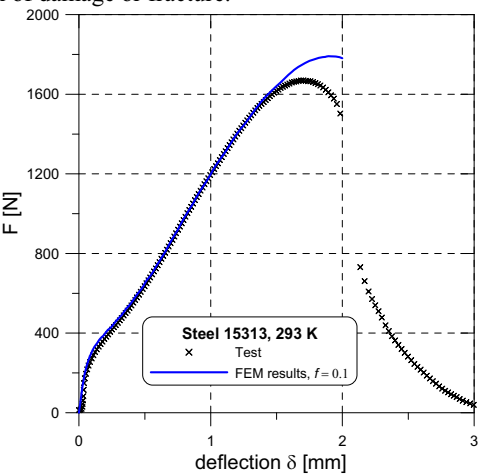

Fig. 4: SPT load deflection diagram for CSN 15313 steel

Results and discussion

Friction in SPT. The contact surface friction between the ball and disc seems to play an important role in the SPT. At room temperature the friction coefficient $f = 0.1$ gives the best fit of our analysis *vs*. experiment (see Fig. 4). The analysis shows that the value of friction coefficient has mainly impact on parts III and IV of the load-deflection diagram [5]. The friction may change dramatically with the surface quality and materials and also vary with the temperature. Load deflection diagrams for all three steels are shown in Fig. 5.

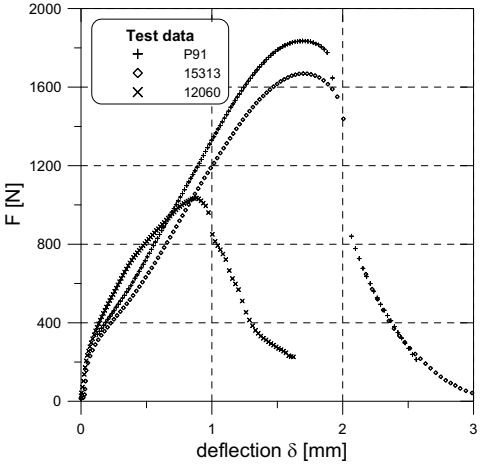

Fig. 5: SPT load-deflection diagram for steels investigated

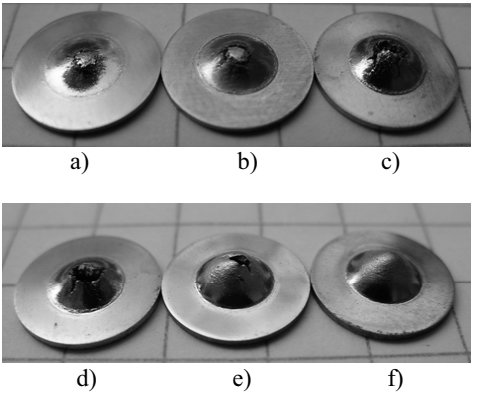

Fig. 6: Development of fracture in various steels:
a) through d) steel CSN 12060 δ = 0.8, 1.0, 1.2 and 1.4 mm,
e) steel CSN 15313 δ = 2.0 mm,
f) steel P91 δ = 2.0 mm

Finarelli *et al*. [6] have tested the influence of various ball materials on the load-deflection curve in CDR tests at room and lower temperatures performed on Eurofer steel. The authors used miniature discs of 3 mm diameter and various thicknesses. "Noisy" failures were observed using the ceramic and sapphire balls and "silent" failures corresponded to steel ball. Apparently, the type of the puncher did not influence the measured SPT curves.

Critical fracture location on the disc. The most critical location from fracture initiation aspect lies generally in localities with the maximum shear stress developing during the deformation process. Such a location tends to move from the specimen center (at small deflections) to about 45 degrees from the symmetry axis (at large deflections). Therefore, discs from CSN 12060 steel tend to rupture from their center and multiple cracks occur in the radial direction from the center as shown in Fig 6a through 6d. Discs from ductile steels (P91 and CSN 15313) usually rupture near 45 degree from the symmetry axis and a circumferential crack often forms a cap that stays attached or detaches from the bursted disc; such crack is already formed in Fig 6f. However, there are cases where the crack initiates from the disc center even in some specimens from ductile materials as shown in Fig. 6e.

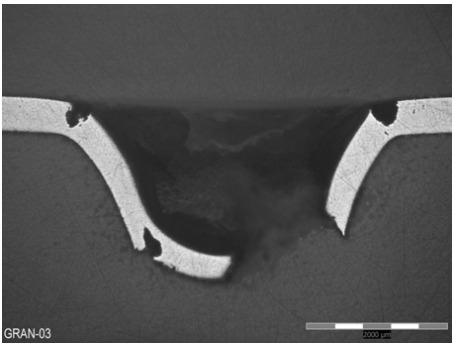

Fig. 7: Section of ruptured disc from CSN 12060

Fig. 8: Section view of ruptured disc from CSN 15313

The brittle damage in SPT is often characterized by cracking on the upper disc surface along the bend circle (see Fig. 7). The discs from ductile materials typically crack in the manner shown in Fig. 8. Bulloch [7] has presented extensive test of various plant components using SPT and observed ductile fracture showing evidence of localized shear process.

At puncher displacement of 1 mm, the equivalent plastic strain (ε_{peq}) over 0.5 was calculated at the most critical location of the disc (~45 degrees), specifically for CSN 15313 steel (see Fig. 9). Such a strain can be considered very high. Probably, the initiation and development of the macroscopic damage would be started in the part III of the load-deflection diagram. The von Misses stress plot for the same location is illustrated in Fig. 10. Macroscopic cracking appeared at deflections around 1.8 mm for this steel; however, micro-cracking can occur earlier in the part III of the load-deflection diagram as was observed by Sainte Catherine *et al*. [8] in A533 B steel.

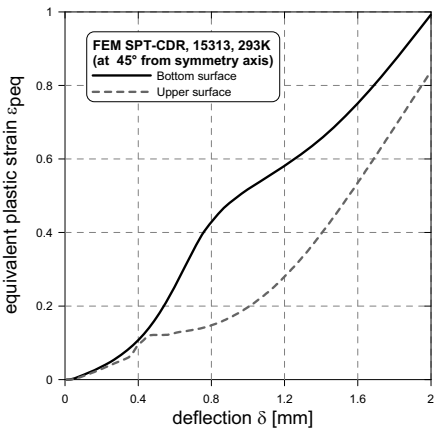

Fig. 9: Equivalent plastic strain *vs*. deflection at most critical disc location

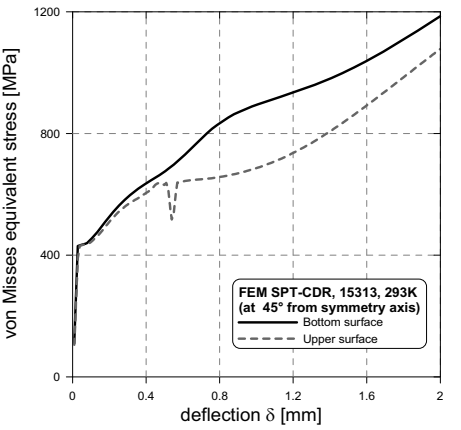

Fig. 10: Von Misses equivalent stress *vs*. deflection at most critical disc location

The SPT curves. The behavior of discs from P91 and CSN 15313 is similar. Contrary to this CSN 12060 shows significantly lower maximum force and deflection at rupture, see the comparison in Fig. 5. According to CWA15627 code [3], the SP fracture energies E_{SP} can be calculated from the area underneath the load-deflection curves. Nominally, the area is defined up to the punch displacement at 20% drop after maximum load. Calculated energies E_{SP} are summarized in Table 5. Significantly low value of E_{SP} was obtained for CSN 12060. Obtained values of SPT energy are in

good agreement with Bulloch [7], who observed fully brittle failure for $E_{SP} < 0.4$ J and fully ductile fracture for $E_{SP} > 1.5$ J depending on temperature in frequently used plant steels.

Table 5: Small punch energy obtained from tests shown in Fig 5

Steel	SP Energy E_{SP} [J]
CSN 15313	1.099
P91	1.149
CSN 12060	0.376

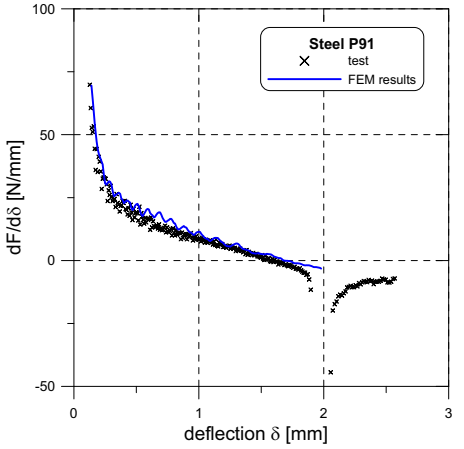

Fig. 11: Force derivative *vs*. deflection for P91

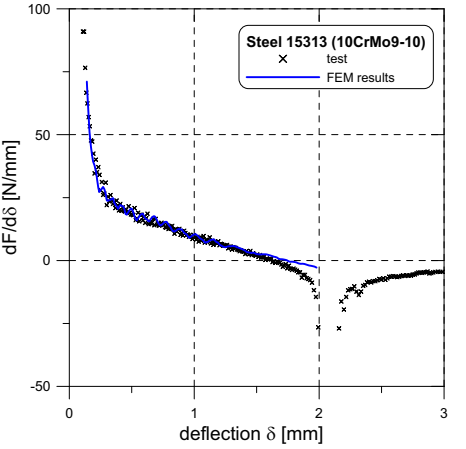

Fig. 12: Force derivative *vs*. deflection for CSN 15313

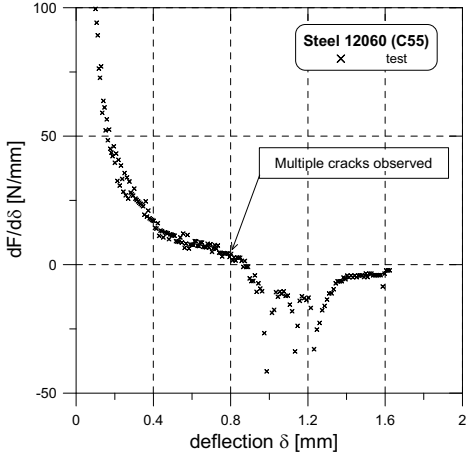

Fig. 13: Force derivative *vs*. deflection for CSN 12060

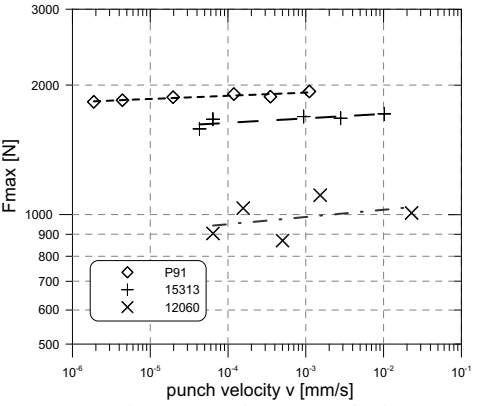

Fig. 14: Maximum SPT force *vs*. velocity

As very useful tool for indication of fracture processes, the analysis of force derivative *vs*. deflection can be considered. This is documented by curves in Figs. 11 through 13. Observed discontinuities, consisting in sudden drop of the derivative, result from instantaneous local fractures. In ductile steels, first three parts of the curve contain no discontinuity, see Figs. 11 and 12, and fracture is localized in the part IV. Contrary to this, multiple discontinuities in the plot are

observed in the parts II and III of the brittle CSN 12060 corresponding to multiple localities of damage. Suitability of formulated FE model is also supported by the fact that experimental derivative bends from the calculated one only when the deflection reaches the vicinity of real fracture.

Note that the observed lower smoothness of the calculated derivative is due to limited number of load steps in FEM.

The dependence of the maximum punch force on punch velocity is illustrated in Fig. 14. Observed great scatter of the test data is typical for brittle steel CSN 12060.

Conclusions

i) The observation and analysis of experimental SPT-CDR curves allow indicating the development of fracture.
ii) Plots of derivative of the force *vs*. deflection seem to be very beneficial tool for detailed analysis of time behavior of the fracture processes.
iii) The applied FE model closely describes the SPT-CDR curves in ductile steels investigated. Contrary to this, the model is probably not applicable in the case of brittle materials due to multiple fracturing of the discs also at very low deflection in these materials.

Acknowledgement

The financial support of the project no. IAA200410801 from the Grant Agency of the Academy of Sciences of the Czech Republic is gratefully acknowledged.

References

[1] K. Milička and F. Dobeš, in: Materials and Technology (Materiali in Tehnologie) 38 (2004) pp. 9–12

[2] T. Kato, T. Nakata, S. Komazaki, Y. Kohno, H. Tanigawa and A. Kohyama: submitted to Mat. Sci. Eng. (2008)

[3] Small Punch Test Method for Metallic Materials CWA15627. Part A: A Code of Practice for Small Punch Creep Testing and Part B: A Code of Practice for Small Punch Testing for Tensile and Fracture Behaviour, Documents of CEN WS21, Brusseles.

[4] M. Abendroth and M. Kuna: Engineering Fracture Mechanics, Vol. 73 (2006), pp 710-725

[5] P. Dymáček, in: New methods of damage and failure analysis of structural parts, TU Ostrava, Czech Republic, September 4-8, 2006, p. 269.

[6] D. Finarelli, F. Carsughi and P. Jung: submitted to Journal of Nuclear Materials (2008)

[7] J.H. Bulloch: Engineering Failure Analysis, Volume 9, Number 5, October 2002 , pp. 511-534

[8] C. Sainte Catherine, J. Messier, Ch. Poussard, S. Rosinski and J. Foulds: In: Small Specimen Test Techniques: Fourth Volume. Edited by M. A. Sokolov, J. D. Landes, G. E. Lucas. American Society for Testing and Materials, West Conshohocken, PA, 2002, p 350.